High Cycle Fatigue Property and Micro Crack Behaviors in Non-combustible Magnesium Alloy

Yasuo Ochi[1, a], Kiyotaka Masaki[2, b], Toshifumi Kakiuchi[1, c], Takashi Matsumura[1, d], Yoshinobu Takigawa[3, e] and Kenji Higashi[3, f]

[1] Department of Mechanical Engineering & Intelligent Systems,UEC,Tokyo, (Universty of Electro-Communications, Tokyo),Chofu,Tokyo,182-8585,Japan

[2] Department of mechanical Systems Engineering, Okinawa Natsional College of Technology, Nago, Okinawa, 905-2192, Japan

[3] Department of Material Science, Osaka Prefecture University, Sakai, Osaka, 99-8531, Japan

[a]ochi@mce.uec.ac.jp, [b]masaki-k@okinawa-ct.ac.jp, [c]kakiuchi@mce.uec.ac.jp, [d]matu@mce.uec.ac.jp, [e]takigawa@mtr.osakafu-u.ac.jp, [f]higashi@mtr.osakafu-u.ac.jp

Keywords: High cycle fatigue, Micro crack initiation site, Crack propagation behavior, Magnesium alloy, Non-combustible

Abstract. High cycle fatigue tests with rotating bending loading were carried out at room temperature on the non-combustible magnesium alloy AMCa602, which was produced by adding 2% Ca to the Mg-Al-Mn system magnesium alloy. The fatigue strength at 10^7 cycles was approximately 100MPa. The fatigue property was strongly dependent on the inclusion size. In order to identify the type of the inclusion at the surface crack initiation sites, elemental analyses were conducted by an electron probe microanalyzer(EPMA). The inclusion at the surface crack initiation site was AlN, which may have originated from impurities mixed in during casting. The relation between da/dN and ΔK was analyzed by the surface crack propagation behavior, and the fatigue life was evaluated by using the Paris's law. As a result, it was clarified that most of the fatigue life was spent on crack initiation and micro crack propagation regimes.

Introduction.

Magnesium alloy is the lightest among practical metallic materials and is superior in specific strength, rigidity and recyclability. It is useful for the chassis of electronic devices such as mobiles and notebook computers, and also is expected in automobile parts for weight reduction [1] . However, as magnesium alloy has a highly combustible property, it is not widely used at present[2]. In order to resolve the problem, non-combustible magnesium alloy were developed by adding calcium(Ca)[3-5].By adding Ca, which is more active than Mg, the oxidation reaction of Ca occurs and a coating of calcium oxide is formed on the surface before Mg ignites.

In the present study, high cycle fatigue tests with rotating bending loading were carried out on extruded Mg-Al-Mn system magnesium alloy with adding 2% Ca, AMCa602 to investigate the

fatigue property of the alloy and the surface micro crack initiation and propagation behaviors. And the crack initiation sites were identified by using an electron probe microanalyzer(EPMA).

Material and Experimental Procedures

The test materials used is the extruded non-combustible magnesium alloy AMCa602. The chemical composition is shown in Table 1. The alloy contains approximately 6% of Al, and 2% added of Ca to the AM60 alloy for combustion resistance. The extrusion conditions of the alloy are shown in Table 2. In the extrusion process, a round bar of φ16mm were prepared. Figure 1 shows the microstructure of a plain parallel to the extrusion direction. In the alloy, the grain size is approximately 30μm. It was observed that inclusions exist in a discontinuous manner parallel to the extrusion direction. The mechanical properties of the alloy are shown in Table 3.

Table 1. Chemical composition of AMCa602t alloy (mass.%)

Al	Ca	Mn	Si	Fe	Cu	Ni	Mg
5.63	2.02	0.281	0.022	0.003	0.005	0.001	Bal.

Table 2. Extruding condition

Output Temp. [K]	Billet Temp. [K]	Extrusion Rate [m/min]	Extrusion Ratio
430	370	2.7	96.3

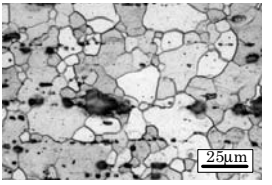

Figure 1. Microstructure of AMCa602 alloy

Table 3. Mechanical property of AMCa602 alloy

Young's modulus, E/GPa	Tensile strength, σ_B/MPa	0.2% Proof stress, $\sigma_{0.2\%}$/MPa	Elongation (%)	Vickers Hardness Hv
40	273	203	9	57

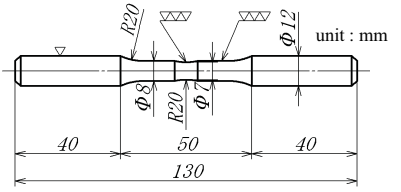

Figure 2. Shape and dimension of fatigue test specimen.

Figure 2 shows the configuration of the fatigue test specimen. The stress concentration factor at the center of the test specimen was 1.05. The mirror finish was given at the center of the specimen surface by wet polishing using emery paper of #2000 with kerosene, followed by buffing. The high cycle fatigue tests with rotating bending loading in a frequency of 2760rpm at a stress ratio R=-1.0 carried out in air at room temperature. In order to investigate the crack initiation and the propagation

behaviors, successive observations of the surface were performed using a plastic replication technique during the fatigue tests. Moreover, the fracture surface of the specimen after the fatigue tests were observed by an electron scanning microscopy (SEM), and the inclusions as the crack initiation sites were identified by using a electron probe microanalyzer(EPMA). These experimental methods and conditions are similar to those of the previous study on the exrtrudedAZ31 magnesium alloy by the present authors[6].

Experimental Results

Figure 3 shows the S-N diagrams obtained in the present study. The experimental data did not disperse comparatively.From the figure, the fatigue strength of the AMCa602 alloy is approximately 100MPa. In the figure, the experimental data of the AMCa602B alloy by Y.Kitahara et al.[7] are plotted. Comparing with the AMCa602B to the present alloy, the fatigue strength at 107 cycles of the AMCa602B is a little higher, and the variation of the fatigue life in the AMCa602B is larger than that of the present alloy.

Figure 4 shows the fracture surfaces after the applied stress amplitude of 130MPa and 110MPa. It was easy to indentify the crack initiation sites by the SEM observation, and those were inclusions near surface from the observations. The sizes of the inclusions at the crack initiation sites were around 100μm in diameter. On the other hands, in the study by Y.Kitahara et al.[7], the size of the inclusions were smaller(around 50μm). Then, it is assumed that the difference in size of inclusions at the crack initiation sites in the both alloys, is one of the factors leading to the difference in the fatigue strength. Besides the inclusions near the fracture initiation sites, other bright areas were observed in the SEM images. The size of the bright area were dependent on the applied stress amplitude.

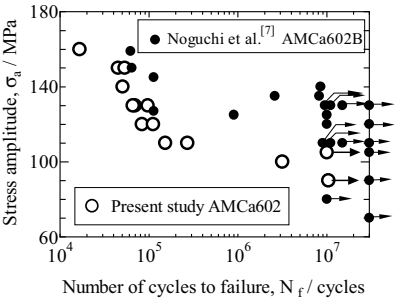

Figure 3. S-N diagrams of AMCa602 and AMCa602B alloys

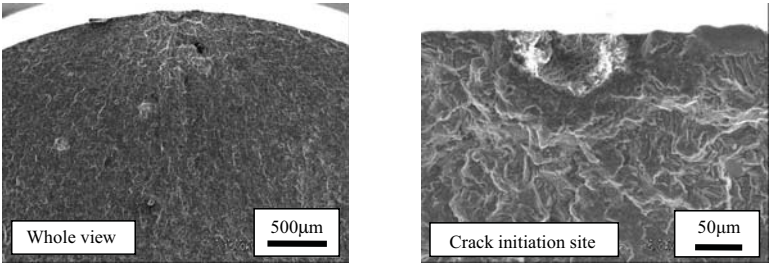

(a) σ_a=130 MPa, N_f=6.6×10^4 cycles.

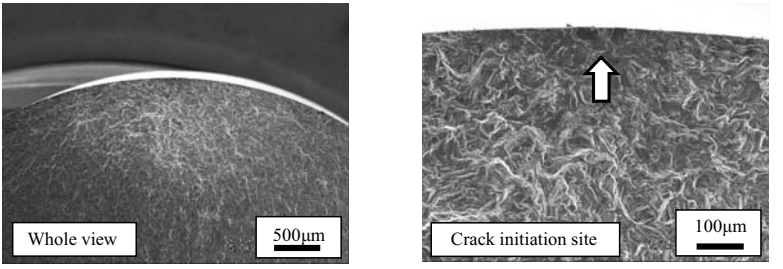

(b) σ_a=110 MPa, N_f=1.5×10^5 cycles.

Figure 4. Examples of fracture surface of AMCa602 alloy

Figure 5 shows the appearance of the surface crack initiation behavior obtained by plastic replication technique. In the figure, it is clearly seen that the crack initiated from the inclusion existing on the surface. Occasionally, the crack did not initiate from the inclusion on the surface but from an inclusion at inside near the surface. The cracks that initiated from the inclusions propagated independently without stopping. Figure 6 shows an example of the crack propagation curve with an applied stress amplitude of 130MPa. It clearly shows that the fatigue crack initiated in an early stage in the fatigue process and the most of the fatigue life was spent on the crack propagation. Figure 7 shows the relation between the crack propagation rate da/dN and the stress intensity factor range ΔK obtained from the Figure 6. For the calculation of theΔK, the equation given by Y.Murakami et al[8] was used. The da/dN-ΔK relation for the AMCa602 alloy has a clear

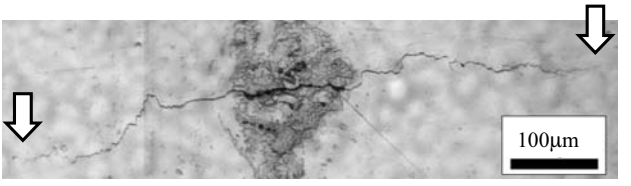

Figure 5. Example of surface crack (plastic replica)

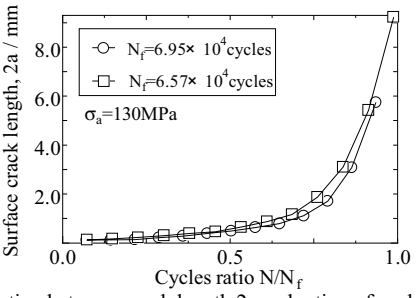

Figure 6. Relation between crack length 2a and ration of cycles to failure N/Nf

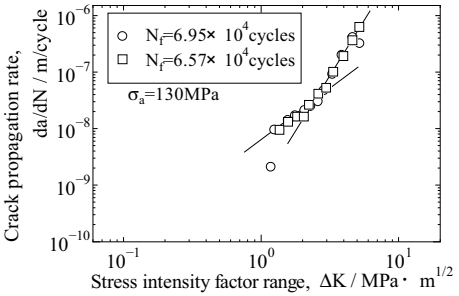

Figure 7. Relation between da/dN and ΔK

Bending point where the stress intensity factor range ΔK is 2.7MPa√m. A bending point in the da/dN-ΔK relation was also observed in the author's previous paper of AZ31[6] and the paper of AZ31 by Tokaji et al[9].

Identification of inclusions at crack initiation sites

From the observations on the surface by replica technique and the fracture surface by SEM, and EPMA analyze, it is clear that there were two types of inclusions as the crack initiation sites. One exists on the surface and the other exists inside near the surface. Figures 8 and 9 show examples of the EPMA analyzed results. Figure 8 shows an inclusion on the surface from which a crack initiated. The Al and N were detected in the inclusion and the Mg, Ca and Mn contents were negligible. Figure 9 shows an inside inclusion near the surface at a crack initiation site. In this case, the inclusion existed at a depth of approximately 100μm from the surface, and the elements detected in the inclusion were the Al and N, as shown as in Figure 8. Consequently, in both the crack initiation types, the inclusions at the crack initiation sites were identified as aluminum nitride, which was used as the material for the metal melting crucible, was mixed in (or produced)[10]. However, the inclusion of the impurities as such is the factor that reduces the actual fatigue strength of the materials, therefore, careful attention should be paid while manufacturing the materials.

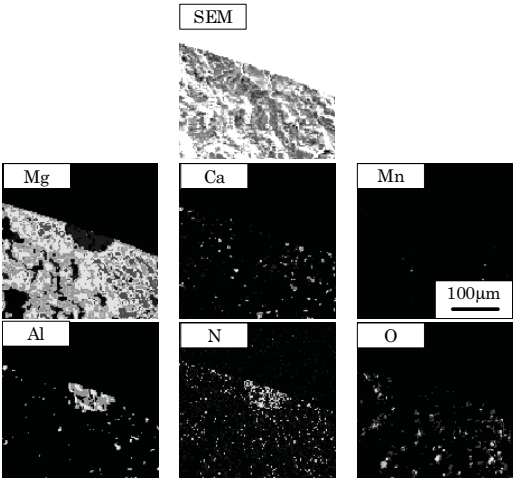

Figure 8. EPMA analyzed results of surface inclusion (σ a=110MPa, N_f=1.5x10^{5}cycles)

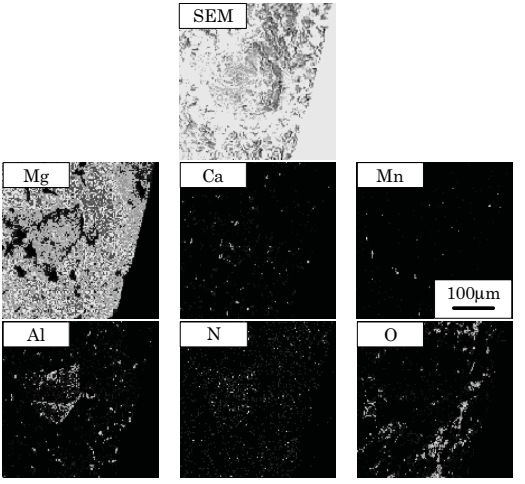

Figure 9. EPMA analyzed results of inside inclusion(σ a=150MPa, N_f=4.5x10^{4}cycles)

Micro crack propagation behaviors

Micro crack propagation behaviors were investigated in the range of a fatigue crack length from the initiation up to the length of 500μm. As described the former section, the fatigue crack initiated from comparatively large size inclusions of aluminum nitride in the most specimens. Figure 10 shows examples of observation results by replication technique on the specimen surface and the early propagation behaviors of the micro cracks with the stress amplitude of 130MPa. Figure 10(a) shows

the case of crack from a large inclusion, and Figure 10(b) shows the case from a small inclusion. When the size of the inclusion at the crack initiation site was large, it was observed that the crack propagation rate of about 10^{-8} m/cycles immediately after the crack initiation. On the other hand, when the crack initiated from a small inclusion, the crack propagation rate was about 10^{-10} m/cycles shortly after the crack initiation. In the latter case, the propagation rate gradually increased along with the crack propagation, and when the crack length 2a=200μm, the crack started to propagate at a constant rate of approximately 10^{-8} m/cycles. That is say, even if the crack initiation site was a large inclusion of approximately 100μm in diameter, the crack propagation behavior after the crack length became 2a=200μm was that of original properties of the AMCa602 alloy. At a crack length 2a=200μm under a stress amplitude of 130MPa, the stress intensity factor is approximately 1.5MPa√m, which precedes the bending point shown in Figure 7.

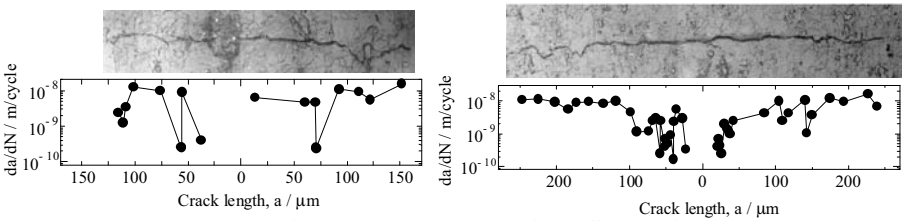

(a) Large size inclusion case (b)Small size inclusion case

Figure 10. Microscopic observation and crack propagation rate of small surface fatigue crack

There is a clear bending point in Figure 7.which shows the relation between the crack propagation rate da/dN and the stress intensity factor range ΔK. In the previous study on AZ31, the appearance of this bending point was explained as being because the crack propagation path changed when the size of the plastic zone at the crack tip, which is dependent on the ΔK, became larger than the grain size[6]. Before the bending point, the crack propagation path was intergranular, and after that, the path became transgranular. In the former case, the fracture surface exhibited a rough morphology, while in the latter case, the fracture surface exhibited a flat morphology. With the change in the crack propagation path, the crack propagation rate changed such that the bending point appeared in the da/dN-ΔK curve. To investigate whether this applies to AMCa602 alloy as well, the plastic zone size at the crack tip was calculated and compared with the grain size. The relation between the plastic zone size r_p and the ΔK is expressed by the following equation[11].

$$r_p = \frac{1}{2\pi}\left(\frac{\Delta K}{\sigma_y}\right)^2$$

Substituting ΔK=2.7MPa√m and σ_y(yield stress)=203MPa, which is the 0.2% proof stress of AMCa602 alloy, the plastic zone size r_p was calculated as 28μm. The average grain size of the AMCa602 alloy used in the study was approximately 12μm. Grain with sizes ranging from 10μm or less to approximately 30μm coexisted. The plastic zone size of 28μm estimated in the above

calculation is approximately equal to the maximum grain size. When the stress amplitude are 110MPa and 130MPa, the half crack length with which the ΔK is 2.7MPa√m and the bending point are 1020μm and 680μm, respectively.

Summary

The high cycle fatigue tests with rotating bending loading were carried out on the extruded non-combustible magnesium alloy AMCa602. The main conclusions are summarized as the followings,

(1) The fatigue strength of the AMCa602 alloy at 10^7 cycles was approximately 100MPa.

(2) The crack initiation sites in the alloy were inclusions of aluminum nitride on the surface or inside near the surface. And, the inclusions affect the crack initiation and micro crack propagation till the crack length reaches 2a=200μm.

(3) In the da/dn-ΔK relation, a clear bending point exists near at the ΔK=2.7MPa√m. The reason why the bending point appears is that when the size of the plastic zone size at the crack tip exceeds the grain size.

(4) Most of the fatigue life of the alloy was spent on the micro crack propagation, which was the regime until the ΔK reached 1-2MPa√m.

References

[1] Y.Murakami and K.Kamei: Non-Ferrous Metallic Materials (Asakura shoten, Tokyo,1978)

[2] S.Nemoto:Shoho kara manabu magnesium, Ichiban karui kinzoku kozozai (Kogyo Chosakai Publishing Co.,Ltd,Tokyo,2002)pp.187-190.

[3] S.Akiyama: J. of JFS 66(1994)pp.38-42.

[4] M.Sakamoto, S.Akiyama, T.Hagioand K.Ogi: J of JFS 69(1997)pp.227-233.

[5] S.Akiyama, H.Ueno and M.Sakamoto: J of JFS 72(2000) pp.521-524.

[6] Y.Ochi, K.Masaki, T.Hirasawa, X.Wu, T.Matsumura, Y.Takigawa and K.Higashi: Material Trans.,47(2006)pp.989-994.

[7] Y.Kitahara, K.Ikeda, H.Shimazaki, H.Noguchi, M.Sakamoto and H.Ueno: Trans. Jpn. Soc. Mech. Eng. A 72(2006)pp.661-668.

[8] Y.Murakami: Stress Intensity Factors Handbook, (Pergamon Press, U.K.1987)p.657.

[9] K.Tokaji, M.Kamakura, Y.Ishizuka and N.Hasegawa: Int. J. of Fatigue, 26(2004)pp.1217-1377.

[10] N.Hotta, I.Kimura, K.Ichiya, N.Saito, S.Yasukawa, K.Tada and T.Kitamura: J.Cera. Soc. Jpn. 96 (1988) pp.731-735.

[11] A.J.McEvily and Z.Yang: Met. Trans.A 21A (1990) pp.2717-2727.